

Linear Viscoelastic Behavior of Nano-Modified Bitumen-Filler Mastics with Different Mineral Fillers

Banreddy Harish¹, Dr. C. Sashidhar², Dr. C. Ramachandrudu Chittar³

- 1 Research Scholar, Department of Civil Engineering, JNTUA, Ananthapuramu, Andhra Pradesh.
- 2 Professor, Department of Civil Engineering, JNTUA College of Engineering, Ananthapuramu, Andhra Pradesh.
- 3 Principal, CRIT, Ananthapuramu, Andhra Pradesh.

Abstract : This study investigated the linear viscoelastic (LVE) behavior of nano-modified bitumen-filler mastics incorporating different mineral fillers and nano-additives. Bitumen-filler mastics were prepared using three commonly used mineral fillers—Granite Filler (GF), Limestone Filler (LSF), and Marble Powder Filler (MPF)—at varying filler-to-binder (F/B) ratios of 0.6, 0.8, and 1.2. To enhance the performance of these mastics, three nano-modifiers—nanoclay (NC), nano-silica (NS), and nano-titanium dioxide (NT)—were incorporated at a fixed dosage of 3% by binder weight. One viscosity grade (VG) bitumen binder i.e., VG40, was used. The rheological properties of the mastics were evaluated using a Dynamic Shear Rheometer (DSR) following EN 14770 standards. Amplitude sweep tests were performed to determine the LVE limits, followed by temperature-frequency sweeps across a temperature range of 15 °C to 70 °C and frequency range of 0.1–100 rad/s. The complex shear modulus (G^*) and phase angle (δ) were obtained to characterize the viscoelastic performance. The LVE regime was compared against SHRP-defined limits for shear strain (γ LVE) and shear stress (τ LVE). The results indicated a consistent exponential decay in LVE strain with increasing G^* , across all filler types, nano-modifiers, and F/B ratios. Among the nano-additives, nanoclay-modified mastics exhibited the most significant improvement in maintaining a broader LVE range, followed by nano-titanium and nano-silica. NT-modified mastics showed superior correlation with SHRP models in LSF and GF systems, whereas NC performed best in MPF systems. A generalized exponential relationship between G^* and LVE strain was developed for all combinations, enabling to predict LVE-region and understand the viscoelastic behavior across a wide spectrum of bitumen-filler mastics. This study demonstrated the effectiveness of nano-modifiers in enhancing the stiffness and LVE performance of bituminous mastics for pavement applications.

IndexTerms - Nano modifiers, marble powder filler, bitumen-filler mastic, linear viscoelastic, dynamic shear rheometer.

I. INTRODUCTION.

The durability and structural performance of flexible pavements largely depend on the characteristics of Hot Mix Asphalt (HMA), with the bitumen-filler mastic playing a central role. This mastic, formed by combining bitumen with mineral fillers and fine aggregates, significantly influences the mixture's resistance to deformation, fatigue, and thermal stress. Critical factors affecting mastic behavior include the filler-to-binder ratio, the type and nature of the filler, and the bitumen's inherent properties. Recent material innovations, particularly in nanotechnology, have opened new avenues for improving mastic performance. Nano-additives like nano-silica, nano-clay, and nano-alumina enhance stiffness, reduce thermal susceptibility, and strengthen rutting and cracking resistance when evenly dispersed. At the same time, there is increasing interest in environmentally friendly alternatives to traditional fillers. Waste marble powder, a by-product of the marble industry, presents itself as a viable option due to its fine particle size and abundant supply. However, limited research exists on the combined effects of nano-modifiers and marble powder in asphalt mastic formulations.

This study focuses on evaluating how marble powder and selected nano-materials influence the rheological and mechanical response of asphalt mastics. It aligns with the broader move toward performance-based material assessments that rely on intrinsic properties rather than empirical methods. Testing tools like the Dynamic Shear Rheometer (DSR) and Bending Beam Rheometer (BBR) are employed to assess parameters such as complex modulus, fatigue behavior, and thermal cracking resistance under varied conditions. In addition to aiming for technical advancements, the research supports sustainability by promoting the use of industrial waste as filler material, thereby reducing dependence on natural resources and minimizing environmental impact. Ultimately, this work seeks to deliver practical insights for engineers and decision-makers aiming to design long-lasting, eco-friendly pavements using optimized mastic formulations.

Mansoori and Modarres (2020) examined the effects of a newly formulated chemical warm mix additive, PAWMA, on the rheological and microstructural properties of bituminous mastics. Compared to Sasobit and Zycotherm, PAWMA showed promise in reducing mixing temperatures without degrading mechanical performance. AFM analysis indicated that PAWMA and Zycotherm preserved mastic morphology, while Sasobit caused noticeable changes in microstructure and surface roughness. The study used a base binder of 60/70 penetration grade and limestone filler at 60% by bitumen weight.

Xing et al. (2020) also explored how fiber morphology affects asphalt mastic performance. Four fibers were studied—lignin and sepiolite (floculent), and basalt and aramid (bundle-type). Floculent fibers mainly enhanced structural stability, while bundle fibers improved toughness and flexibility. Regardless of type, all fibers improved rutting resistance, suggesting their utility in enhancing pavement durability.

Motevalizadeh and Mollenhauer (2024) assessed how filler mineralogy and asphalt technologies influence ageing in bituminous mastics. Limestone, basalt, and diabase fillers were tested with various binder types. Ageing effects were evaluated through shear rheology and FTIR spectroscopy, with carbonyl and sulfoxide indices quantifying oxidation. GSCS and Hashin models estimated immobilized binder volumes. Data were analyzed using PLSR and HCA, which grouped mastics into four clusters based on combined chemical and mechanical properties. Limestone fillers, especially with foamed bitumen, offered the best ageing resistance.

Shabani et al. (2024) developed the ARCTIC test to evaluate low-temperature cracking in bitumen and mastics using a restrained cooling approach. This method provides a simpler alternative to complex lab tests. Two bitumen types and their mastics were tested, and the results showed high repeatability. Finite element modeling supported the physical tests, helping to calculate thermal stress and fracture parameters. The ARCTIC test was shown to effectively assess low-temperature performance, making it suitable for routine material evaluation.

II . MATERIALS AND METHODOLOGY.

Preparation of bitumen-filler mastics.

In this study, an extensive laboratory program was carried out to develop bitumen-filler mastics incorporating both mineral fillers and nano-scale additives. The primary goal was to assess how different filler types and nanomaterials affect the linear viscoelastic (LVE) behavior of these mastics when combined with various asphalt binders. Three mineral fillers—Granite Filler (GF), Limestone Filler (LSF), and Marble Powder Filler (MPF)—were selected for their distinctive physical and chemical properties, which are known to influence binder interaction. These fillers are widely utilized in pavement construction due to their accessibility, economic feasibility, and diverse mineralogical compositions, allowing for a controlled comparative study of their effects on mastic behavior under uniform conditions.

To improve the functional performance of the mastics, three nano-modifiers were used: nano-silica (NS), nano-titanium dioxide (NT), and nanoclay (NC), each added at 3% by binder weight. These nanomaterials were chosen based on their ability to enhance asphalt mixtures—nano-silica offers improved stiffness and thermal stability through its high surface area and bonding potential; nano-titanium provides UV resistance and enhances durability; and nanoclay contributes to aging resistance and barrier properties due to its layered microstructure.

The study utilized one type of unmodified asphalt binders—VG-30—which is standard in road construction and provide baseline rheological characteristics. For mastic preparation, the mineral fillers were first oven-dried and weighed based on target filler-to-binder (F/B) ratios. They were then preheated at 180 °C for one hour to remove moisture and ensure thermal uniformity. Simultaneously, the binders were heated to 180 °C for 10 minutes to achieve a workable consistency while minimizing thermal degradation. Nano-additives were either mixed into the binder via high-shear blending or introduced alongside the fillers, depending on their dispersion characteristics.

Rheological characteristics of nano-material based bitumen mastics.

Rheological characterization in this study was conducted using a Dynamic Shear Rheometer (DSR) developed by AntonPaar. Depending on the testing temperature, two plate configurations were employed: a 25 mm diameter parallel plate setup was used for temperatures above 30 °C, while an 8 mm plate was utilized for tests conducted at or below this threshold. The evaluation of both asphalt binders and bitumen-filler mastics adhered to the guidelines provided in the European standard EN 14770.

EN 14770 specifies the method for evaluating the rheological behavior of bituminous binders and their modified forms through DSR testing. It focuses on determining the complex shear modulus (G^*) and phase angle (δ), which collectively describe a material's response to oscillatory shear stress, reflecting its stiffness and viscoelastic characteristics. During the test, the sample is sandwiched between two parallel plates—either 8 mm or 25 mm in diameter—based on the temperature requirements. A preliminary amplitude sweep test is performed to identify the range within which the material behaves linearly (i.e., without structural changes due to applied strain). The plate spacing, or gap, is adjusted to either 1 mm or 2 mm according to the plate size. Finally, the linear viscoelastic range is confirmed, a temperature-frequency sweep is carried out for the following experimental matrix listed in table 1.

Table 1. Experimental matrix for the determination of LVE regime of nano modified bitumen-filler mastics

Component	Type	Dosage
Mineral filler	Marble powder filler (MPF) Limestone filler (LSF) Granite filler (GF)	A filler/binder (F/B) ratio of 0.6, 0.8 and 1.2
Nano-modifier	Nano-clay Nano-silica Nano-titanium	3% by weight of binder
Binder type	VG30 VG40	A filler/binder (F/B) ratio of 0.6, 0.8 and 1.2

The values of LVE regime were compared with the limits given by strategic highway research program (SHRP). The following equations were given by SHRP for the shear strain (γ) and shear-stress (τ) limits for LVE-regime.

$$\gamma_{LVE}(\%) = \frac{12}{G^{*0.29}} \text{ and } \tau_{LVE}(kPa) = 0.12 \times G^{*0.71}$$

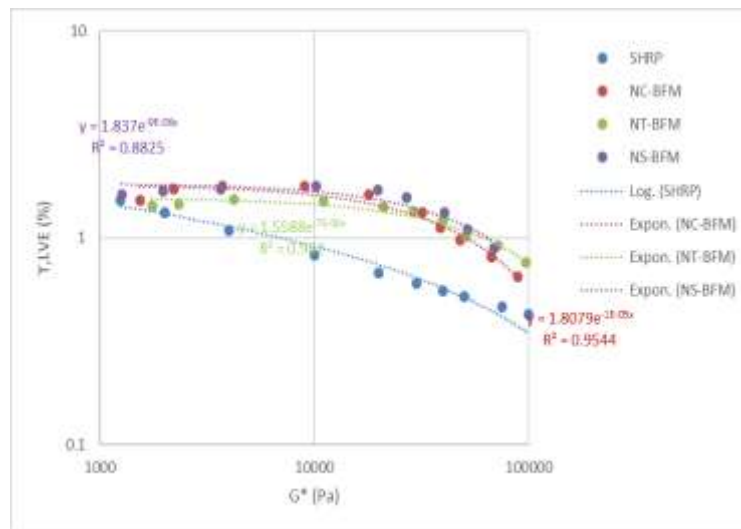


Figure 1. Relation between LVE strain and complex shear modulus for MPF based bitumen-filler mastics at F/B ratio of 0.6

III.RESULTS AND DISCUSSION.

The relationship between the linear viscoelastic (LVE) strain limit and the complex shear modulus (G^*) for marble powder filler (MPF)-based bitumen mastics at a filler-to-binder (F/B) ratio of 0.6 is shown in figure 1. The mastics modified with nanoclay (NC-BFM), nano titanium (NT-BFM), and nano silica (NS-BFM) were compared with the SHRP model. All mastics showed a decrease in LVE strain as G^* increased, indicating a reduction in the linear viscoelastic range with increasing stiffness. While the SHRP model followed a logarithmic trend, the nano-modified mastics exhibited exponential decay. Among them, NC-BFM showed the highest correlation ($R^2 = 0.9544$), followed by NT-BFM (0.9196) and NS-BFM (0.8825), highlighting nanoclay's superior ability to enhance viscoelastic behavior.

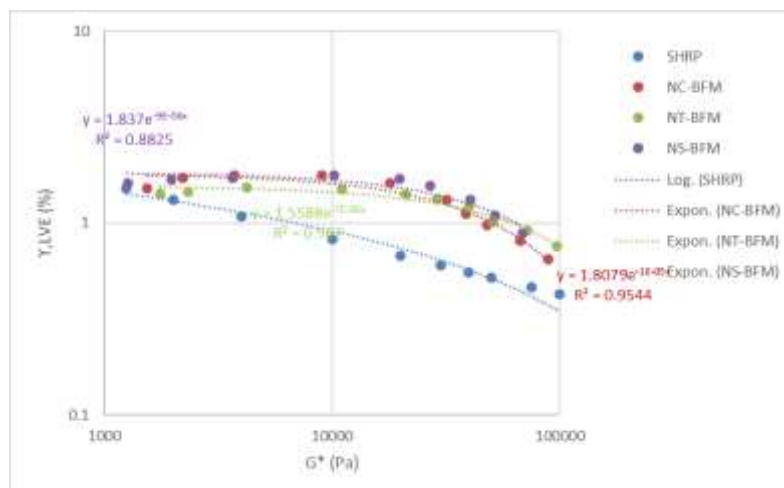


Figure 2. Relation between LVE strain and complex shear modulus for MPF based bitumen-filler mastics at F/B ratio of 0.8

Figure 2 presents the same relationship at a higher F/B ratio of 0.8. The decreasing trend in LVE strain with increasing G^* remained consistent across all mastics. As before, the SHRP model followed a logarithmic decay, while the nano-modified mastics followed exponential decay patterns. NC-BFM again demonstrated the strongest correlation with an R^2 value of 0.9544, reinforcing its

effectiveness in preserving the LVE range at higher filler content. These findings confirm that nanoclay offers the most significant improvement in balancing stiffness and viscoelastic performance in MPF-based mastics.

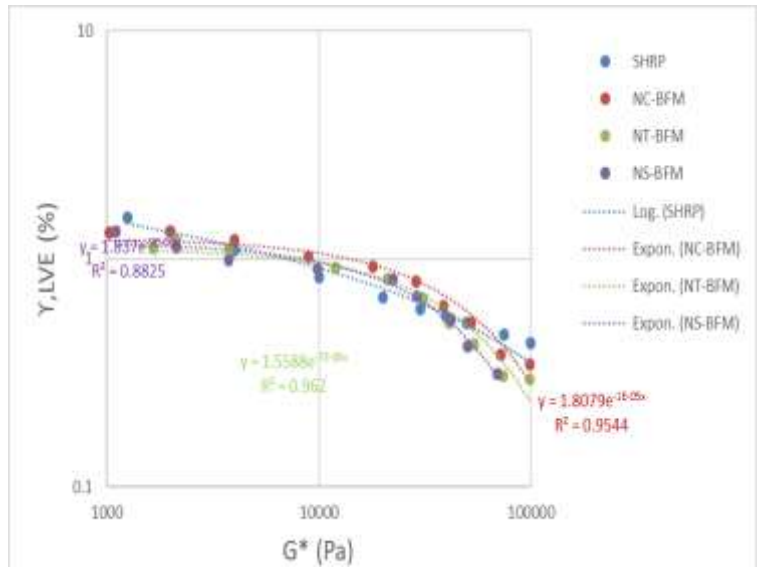


Figure 3. Relation between LVE strain and complex shear modulus for MPF based bitumen-filler mastics at F/B ratio of 1.2

Figure 3 shows the relationship between the LVE strain limit and complex shear modulus (G^*) for MPF-based mastics at a filler-to-binder ratio of 1.2. All mastics, including those modified with nanoclay (NC-BFM), nano titanium (NT-BFM), and nano silica (NS-BFM), exhibited a decreasing trend in LVE strain with increasing G^* , indicating reduced viscoelastic range with higher stiffness. The SHRP model followed a logarithmic trend, while the modified mastics followed exponential decay. Among the nanomodified mastics, NT-BFM showed the strongest fit with an R^2 of 0.962, followed by NC-BFM ($R^2 = 0.9544$) and NS-BFM ($R^2 = 0.8825$). These results highlight nano titanium's superior effect at higher filler content, while nanoclay and nano silica also contributed positively to maintaining viscoelastic behavior.

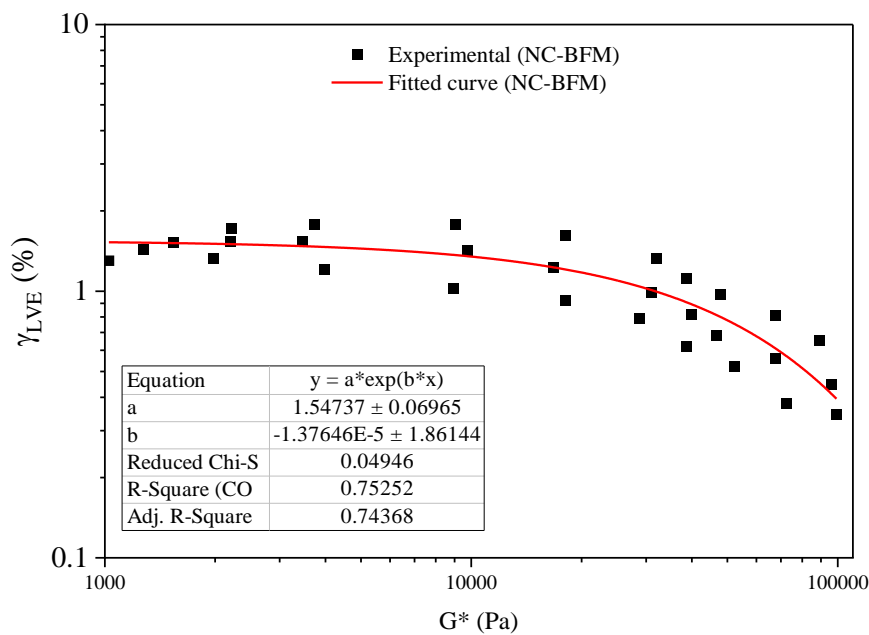


Figure 3.4 Relation between LVE shear strain and complex shear modulus for MPF based bitumen-filler mastics with nano-clay
 Figure 4 showed the relationship between LVE shear strain and complex shear modulus (G^*) for MPF-based bitumen-filler mastics incorporating nanoclay (NC-BFM), covering a range of filler-to-binder (F/B) ratios from 0.6 to 1.2. The experimental data exhibited a decreasing trend in LVE strain with increasing G^* , indicating that higher stiffness limited the strain range over which the material maintained linear viscoelastic behavior. The fitted curve closely followed the experimental points, reflecting a good correlation.

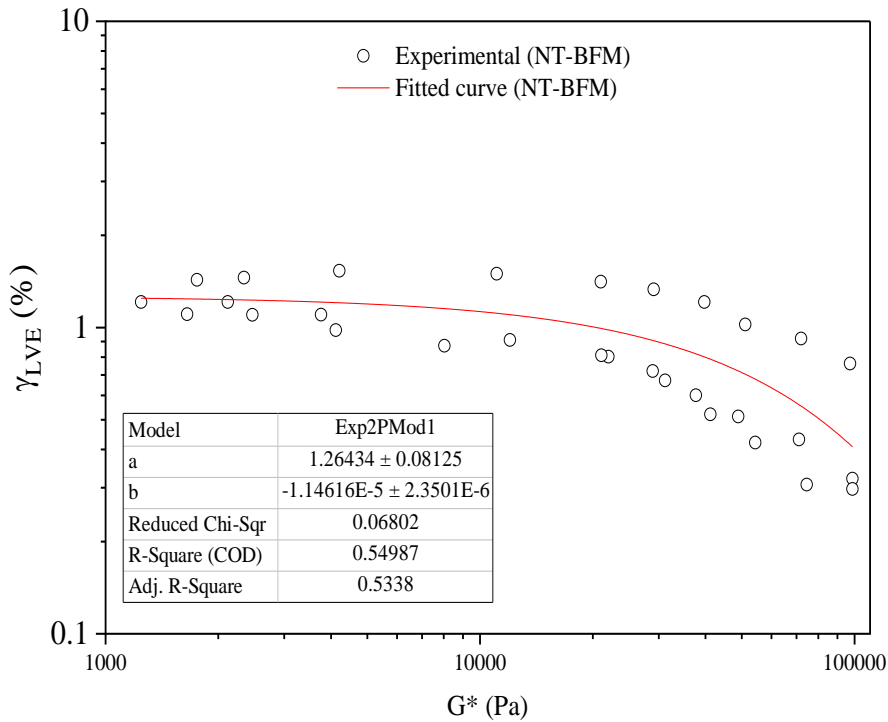


Figure 3.5 Relation between LVE shear strain and complex shear modulus for bitumen-filler mastics with nano-titanium

Figure 5 shows the relationship between LVE shear strain and complex shear modulus (G^*) for MPF-based mastics modified with nano-titanium (NT-BFM) across a filler-to-binder (F/B) ratio range of 0.6 to 1.2. A clear decline in LVE strain was observed with increasing G^* , indicating reduced viscoelastic range as stiffness increased. While the fitted exponential curve aligned with the trend, it exhibited a weaker correlation than nanoclay-modified mastics, suggesting nano-titanium had a limited effect on improving LVE behavior.

Figure 6 presents similar data for nano-silica-modified mastics (NS-BFM) over the same F/B range. The results again showed a decreasing LVE strain with rising G^* , reflecting reduced linear viscoelasticity at higher stiffness levels. The fitted curve showed moderate accuracy, with a better R^2 value than NT-BFM but lower than NC-BFM. These findings indicate that while nano-silica moderately enhances viscoelastic behavior, its impact is less significant than nanoclay but slightly better than nano-titanium.

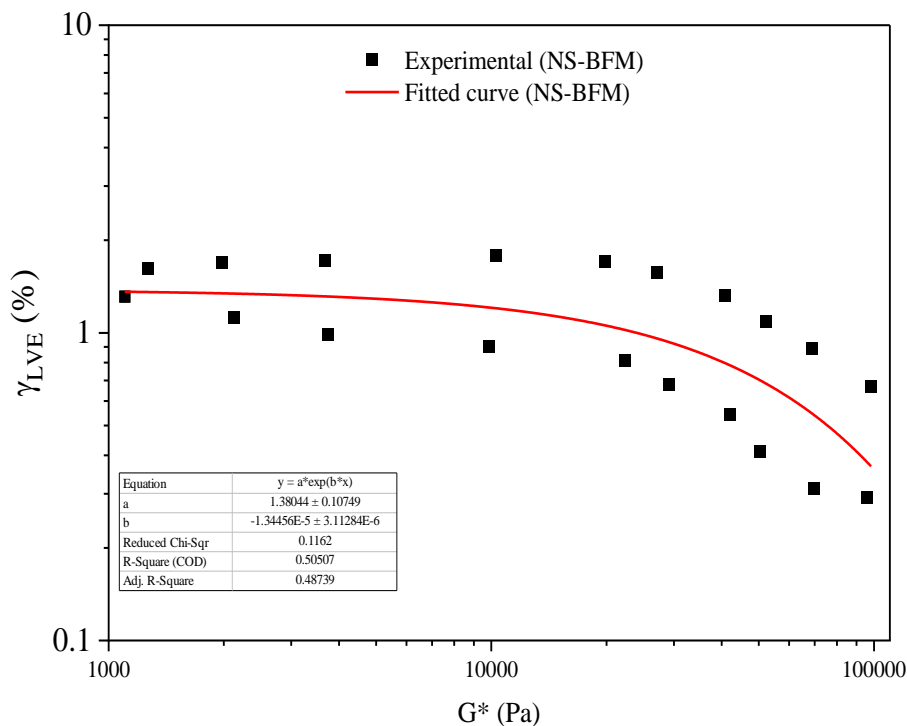


Figure 3.6 Relation between LVE shear strain and complex shear modulus for MPF based bitumen-filler mastics with nano-silica

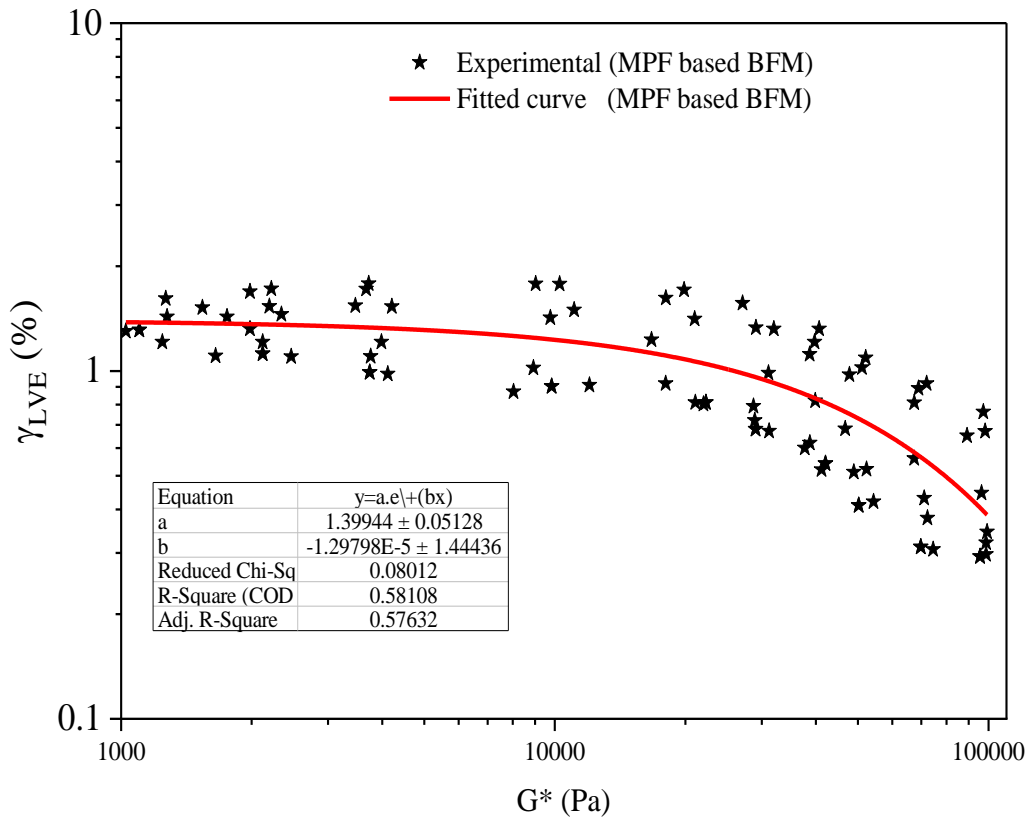


Figure 3.7 Relation between LVE shear strain and complex shear modulus for MPF based bitumen-filler mastics with nano-modifiers.

Figure 7 displays the combined relationship between LVE shear strain and complex shear modulus (G^*) for MPF-based mastics modified with nanoclay, nano-titanium, and nano-silica across F/B ratios of 0.6, 0.8, and 1.2. A consistent decline in LVE strain with increasing G^* was observed, reflecting reduced viscoelastic range with greater stiffness. The data followed an exponential decay trend with moderate correlation, capturing the overall influence of both nano-modifiers and filler content. Despite variations among the additives, the general pattern remained consistent across all conditions.

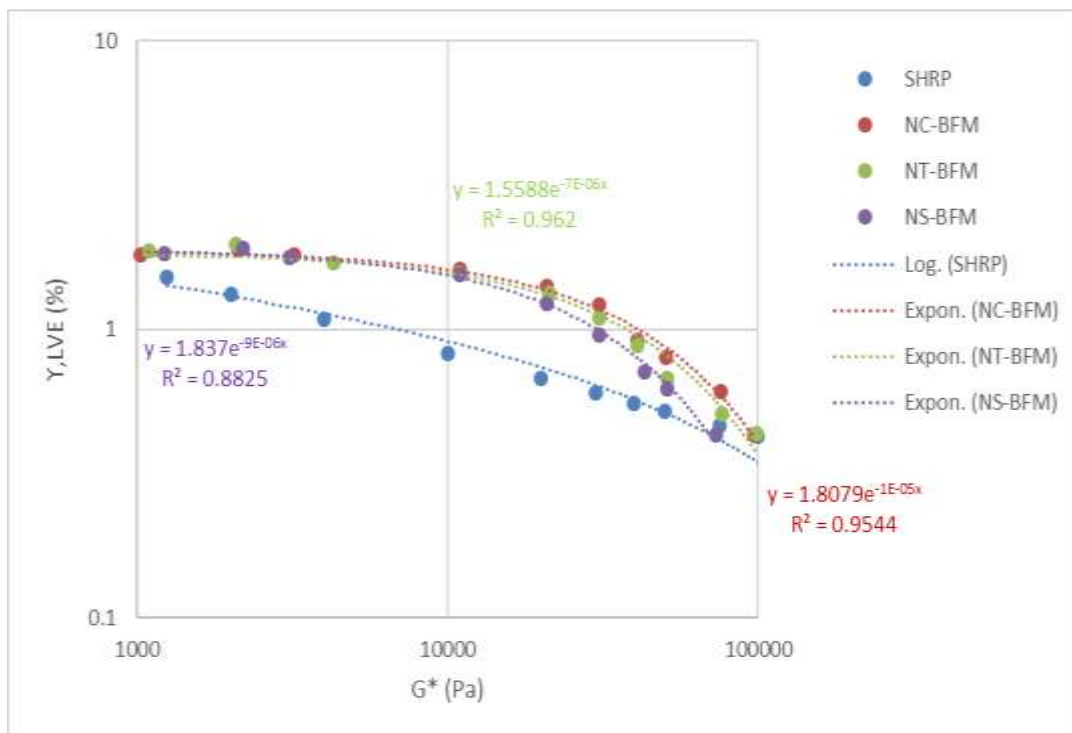


Figure 3.8 Relation between LVE strain and complex shear modulus for LSF based bitumen-filler mastics at F/B ratio of 0.6

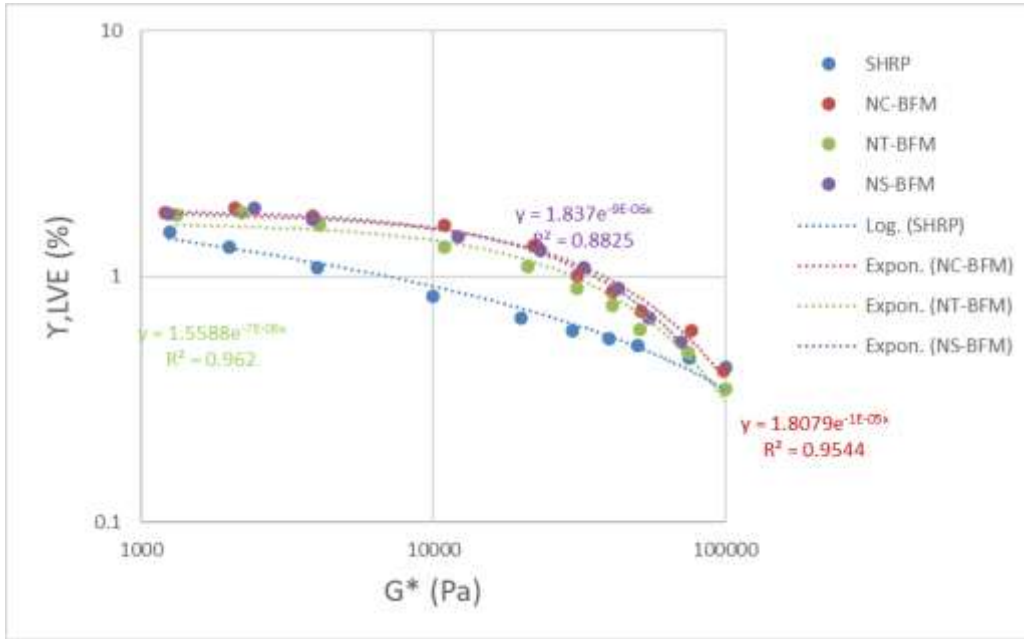


Figure 3.9 Relation between LVE strain and complex shear modulus for LSF based bitumen-filler mastics at F/B ratio of 0.8

Figure 8 illustrates the relationship between LVE strain and complex shear modulus (G^*) for LSF-based mastics at an F/B ratio of 0.6. All nano-modified mastics—NC-BFM, NT-BFM, and NS-BFM—showed an exponential decline in LVE strain with rising G^* , while the SHRP model followed a logarithmic trend. NT-BFM exhibited the strongest correlation ($R^2 = 0.962$), indicating that nano titanium was most effective in maintaining the LVE range at lower filler content.

Figure 9 presents similar results at an F/B ratio of 0.8. A decreasing trend in LVE strain with increasing G^* persisted across all mastics. Again, NT-BFM showed the highest correlation ($R^2 = 0.962$), followed by NC-BFM and NS-BFM, while the SHRP model had the weakest fit. These findings suggest that nano titanium consistently improves strain tolerance and better preserves the viscoelastic range under moderate filler conditions.

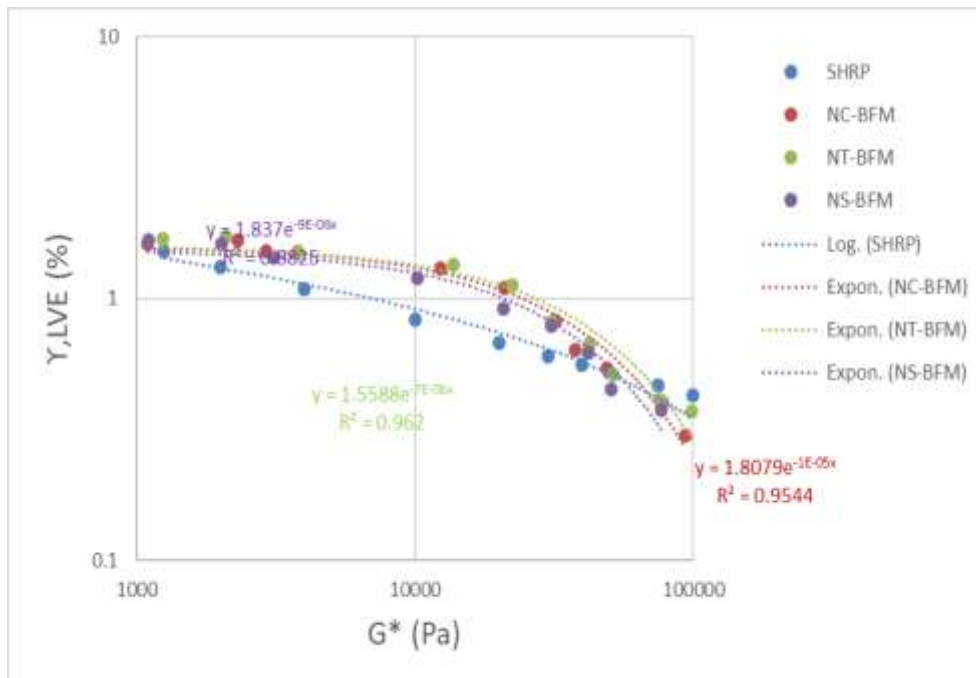


Figure 10. Relation between LVE strain and complex shear modulus for LSF based bitumen-filler mastics at F/B ratio of 1.2.

Figure 10 presents the relationship between LVE strain and complex shear modulus (G^*) for LSF-based mastics at an F/B ratio of 1.2, comparing SHRP's logarithmic trend with exponential fits for nanoclay, nano titanium, and nano silica. All modified systems showed a decline in LVE strain with increasing stiffness. Among them, NT-BFM displayed the strongest correlation ($R^2 = 0.962$), indicating its superior ability to sustain viscoelastic behavior even at higher filler content, followed by NC-BFM ($R^2 = 0.9544$) and NS-BFM ($R^2 = 0.8825$). The SHRP model showed a weaker fit by comparison.

Figure 11 illustrates the effect of nanoclay across all F/B ratios (0.6 to 1.2) in LSF-based mastics. The data confirmed a decreasing LVE strain with rising G^* , consistent with stiffness-induced limitations on viscoelastic performance. The exponential curve fit had an R^2 value of 0.7552, suggesting moderate accuracy. These results indicate that nanoclay supports strain tolerance across varying filler levels, although its effectiveness is less pronounced than nano titanium.

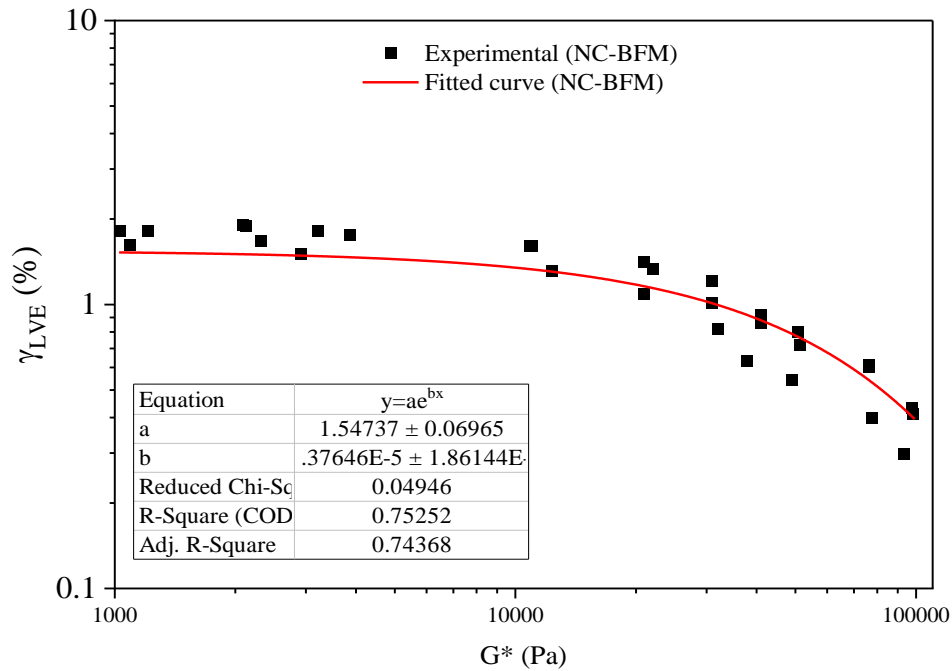


Figure 11 Relation between LVE shear strain and complex shear modulus for LSF based bitumen-filler mastics with nano-clay.

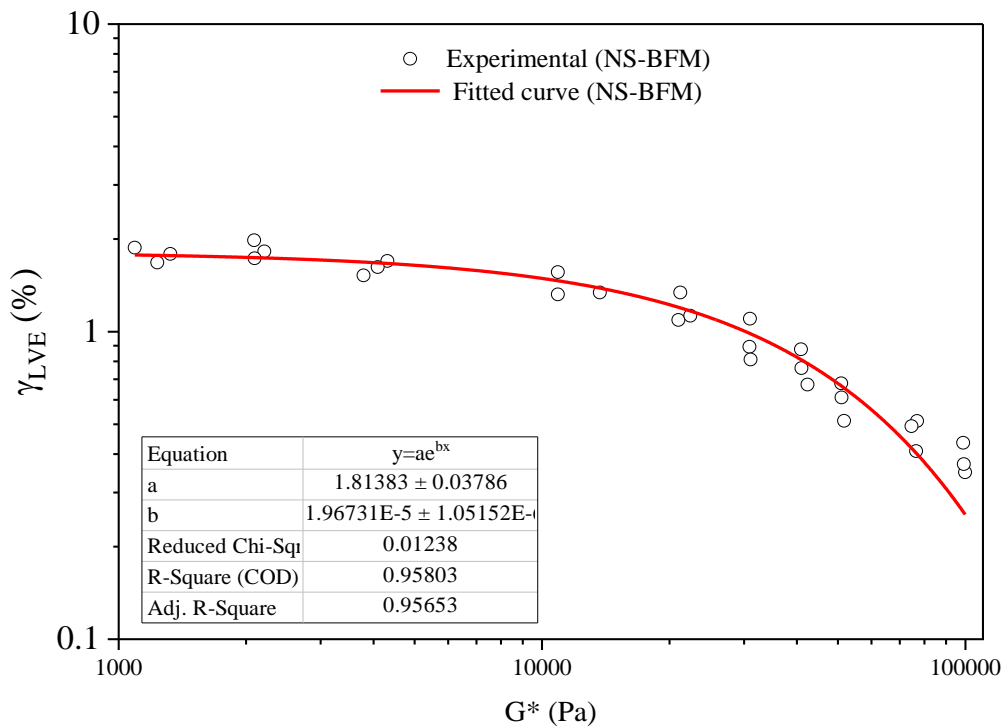


Figure 3.12 Relation between LVE shear strain and complex shear modulus for LSF based bitumen-filler mastics with nano-titanium.

Figure 12 displays the relationship between LVE shear strain and complex shear modulus (G^*) for LSF-based mastics modified with nano-titanium (NT-BFM) across F/B ratios from 0.6 to 1.2. The data showed a clear decline in LVE strain with increasing stiffness, indicating a reduced viscoelastic range. The exponential fit aligned closely with the data, supported by a strong R^2 value of 0.9580 and adjusted R^2 of 0.9563, confirming that nano-titanium provides consistent and reliable enhancement in LVE behavior across varying filler contents.

Figure 13 presents similar findings for mastics modified with nano-silica (NS-BFM) across the same F/B range. A clear inverse relationship was observed, where higher G^* corresponded to lower LVE strain. The exponential curve showed excellent agreement

with the data, also yielding an R^2 of 0.9580 and adjusted R^2 of 0.9563. These results indicate that nano-silica significantly improves viscoelastic response, maintaining strain tolerance effectively over a range of filler levels.

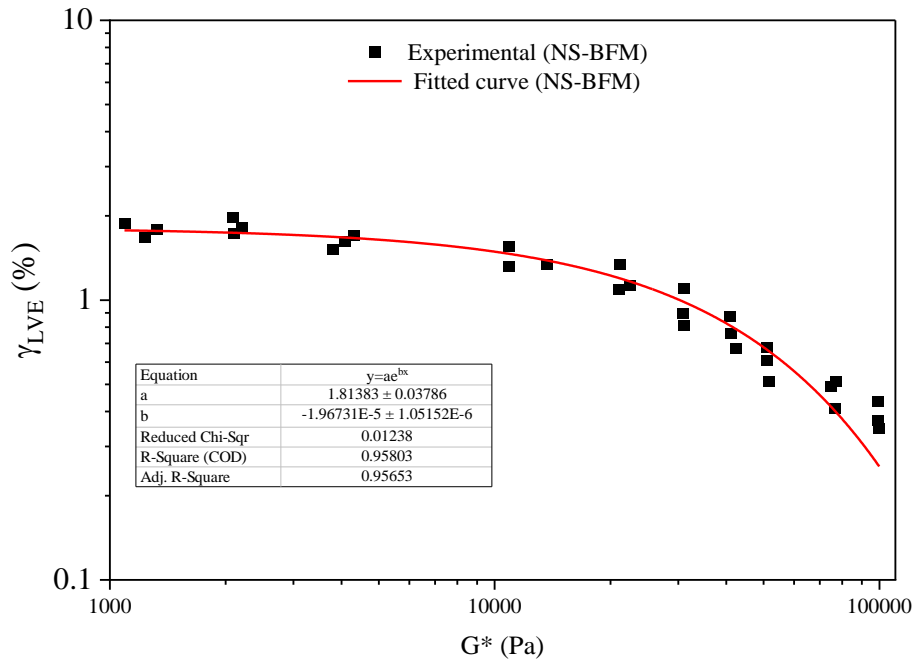


Figure 3.13 Relation between LVE shear strain and complex shear modulus for LSF based bitumen-filler mastics with nano-silica.

Figure 14 shows the relationship between LVE shear strain and complex shear modulus (G^*) for LSF-based mastics incorporating nanoclay, nano titanium, and nano silica across F/B ratios from 0.6 to 1.2. A consistent decrease in LVE strain with increasing G^* was observed, indicating reduced viscoelastic flexibility as stiffness grew. The exponential fit closely matched the experimental data, supported by a strong R^2 value of 0.9413 and adjusted R^2 of 0.9406, highlighting the reliable and predictable impact of nano-modification on viscoelastic behavior across all conditions.

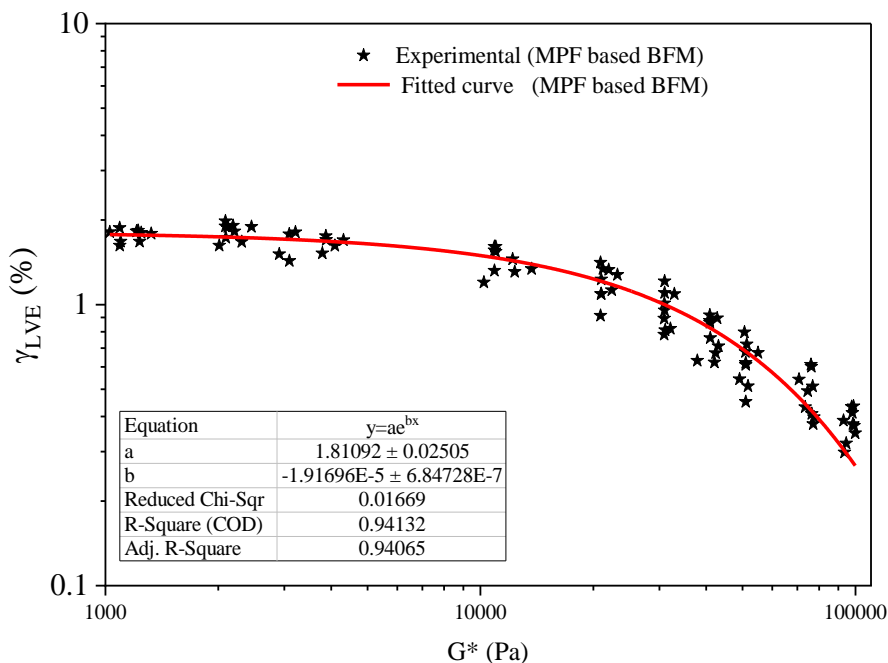


Figure 3.14 Relation between LVE shear strain and complex shear modulus for LSF based bitumen-filler mastics with nano-modifiers.

Figure 15 illustrates similar trends for GF-based mastics at an F/B ratio of 0.6. The SHRP model followed a logarithmic pattern, while nano-modified systems—NT-BFM, NC-BFM, and NS-BFM—exhibited exponential decay in LVE strain with increasing stiffness. Among them, NT-BFM showed the best fit ($R^2 = 0.962$), followed by NC-BFM ($R^2 = 0.9544$) and NS-BFM ($R^2 = 0.8825$). These results indicate that at low filler levels, nano titanium most effectively preserved the linear viscoelastic range in GF-based mastics.

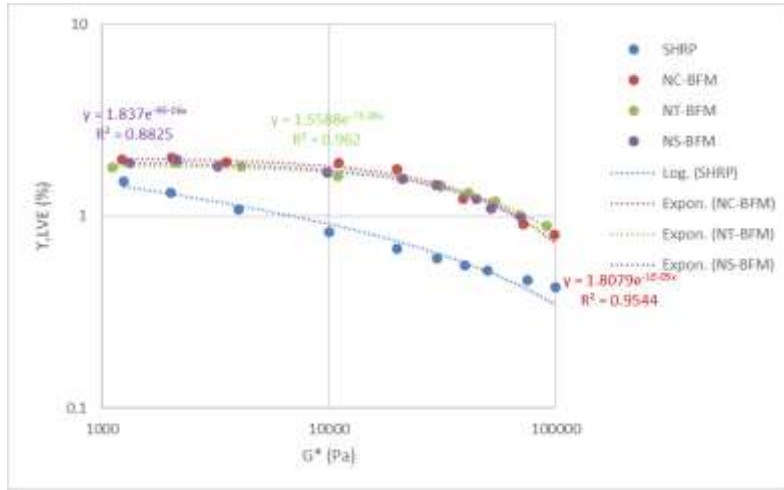


Figure 3.15 Relation between LVE strain and complex shear modulus for GF based bitumen-filler mastics at F/B ratio of 0.6

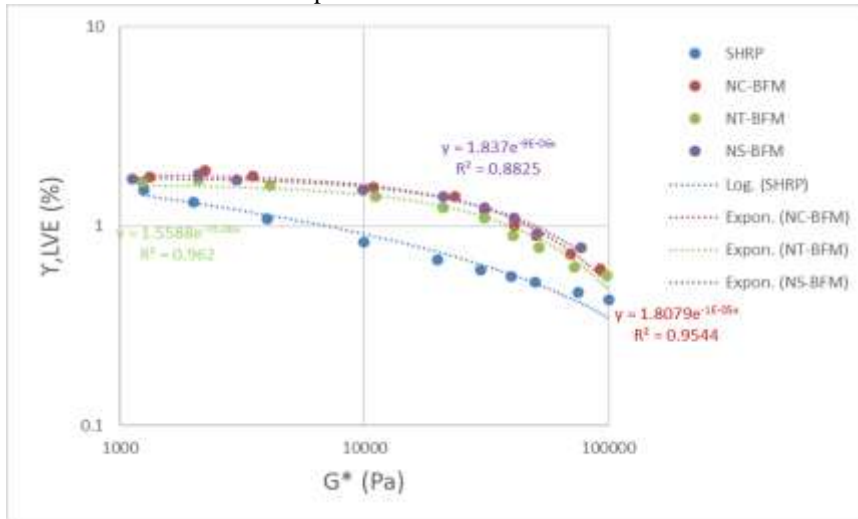


Figure 3.16 Relation between LVE strain and complex shear modulus for GF based bitumen-filler mastics at F/B ratio of 0.8

Figure 16 displays the relationship between LVE strain and complex shear modulus (G^*) for GF-based mastics at an F/B ratio of 0.8. All nano-modified systems—NC-BFM, NT-BFM, and NS-BFM—followed an exponential decline in LVE strain with increasing G^* , while the SHRP model followed a logarithmic trend. NT-BFM showed the strongest fit ($R^2 = 0.962$), followed by NC-BFM (0.9544), while NS-BFM and SHRP had lower correlations ($R^2 = 0.8825$). These findings suggest that nano titanium was most effective in preserving viscoelastic range at this intermediate filler level.

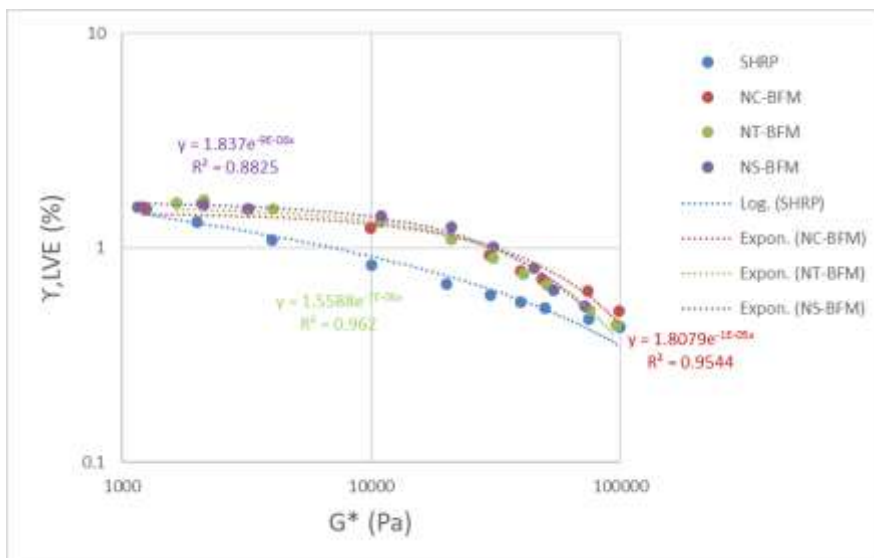


Figure 3.17 Relation between LVE strain and complex shear modulus for GF based bitumen-filler mastics at F/B ratio of 1.2

Figure 17 shows a similar relationship at an F/B ratio of 1.2. Again, all mastics exhibited decreasing LVE strain with increasing stiffness. NT-BFM maintained the highest correlation ($R^2 = 0.962$), indicating its consistent performance across higher filler content. NC-BFM followed with a slightly lower R^2 of 0.9544, while NS-BFM and SHRP remained less predictive. This confirms nano titanium's superior influence in maintaining LVE behavior even at elevated stiffness levels in GF-based mastics.

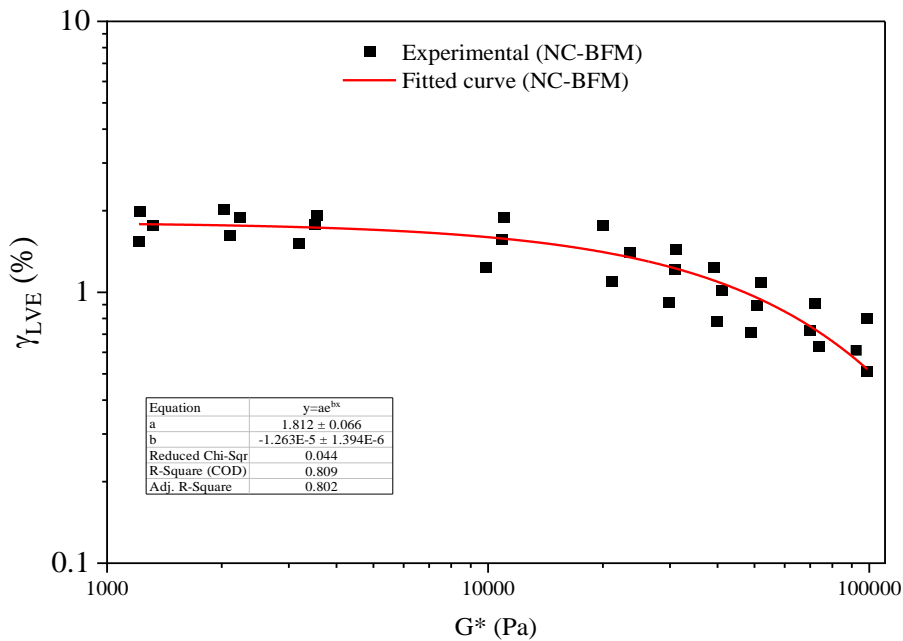


Figure 18. Relation between LVE shear strain and complex shear modulus for GF based bitumen-filler mastics with nano-clay.

Figure 18 presents the relationship between LVE shear strain and complex shear modulus (G^*) for GF-based mastics modified with nanoclay (NC-BFM) across all F/B ratios (0.6, 0.8, and 1.2). The experimental data showed a decreasing LVE strain with increasing G^* , indicating reduced viscoelastic flexibility as stiffness increased. The exponential trend fit moderately well, with an R^2 value of 0.80, suggesting that while nanoclay improved LVE performance, its predictive strength was limited compared to other nano-modifiers.

In contrast, Figure 19 illustrates the same relationship for GF-based mastics modified with nano-titanium (NT-BFM). The data exhibited a consistent inverse trend between LVE strain and G^* , with the exponential fit showing stronger agreement ($R^2 = 0.887$). These results confirmed that nano-titanium offered better enhancement of LVE properties than nanoclay, providing improved consistency and strain tolerance across varying filler levels and stiffness conditions.

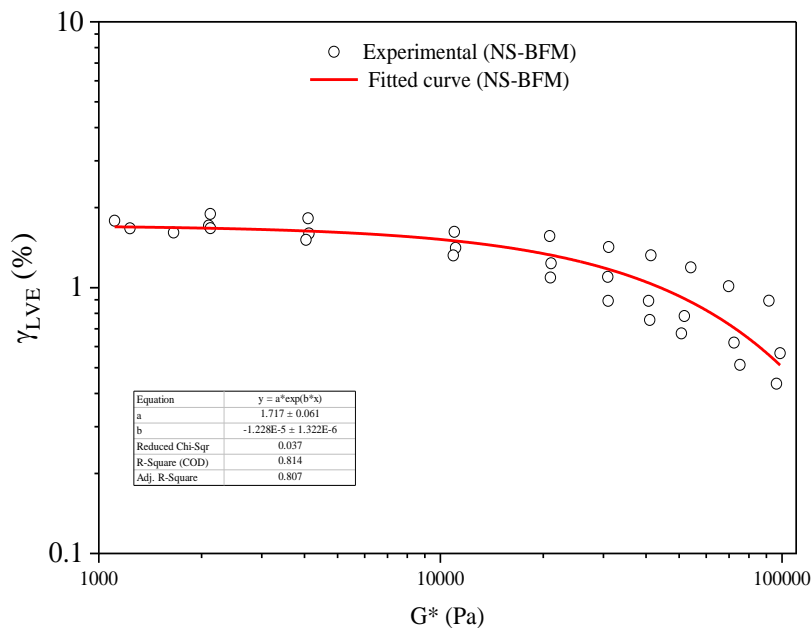


Figure 19. Relation between LVE shear strain and complex shear modulus for GF based bitumen-filler mastics with nano-titanium.

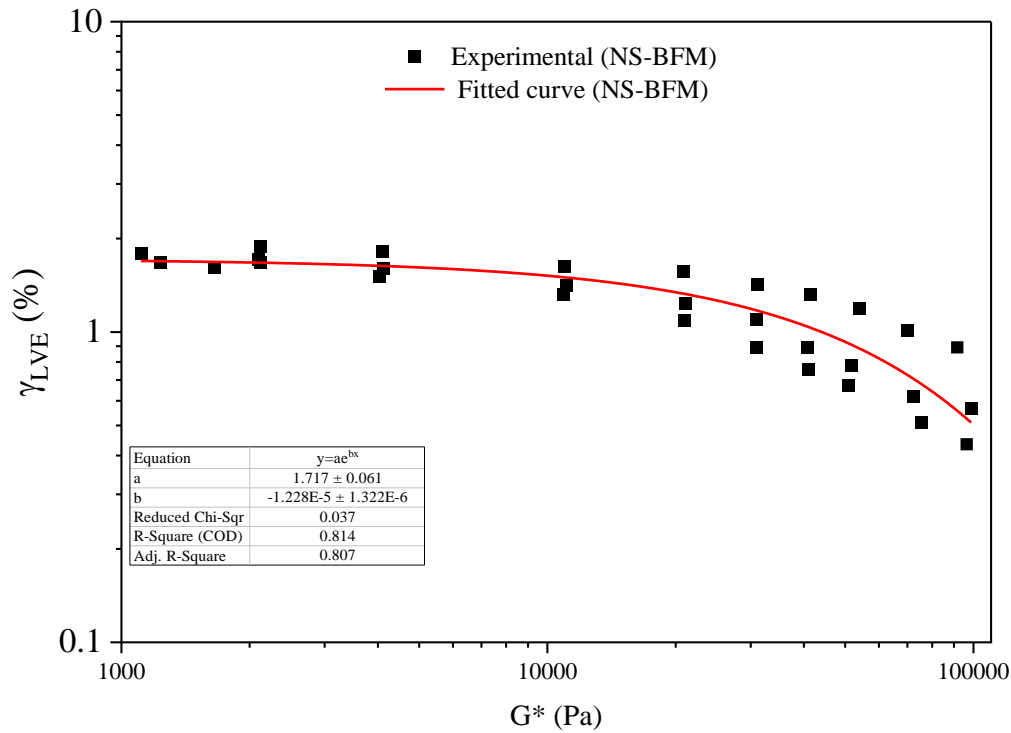


Figure 20. Relation between LVE shear strain and complex shear modulus for GF based bitumen-filler mastics with nano-silica.

Figure 20 presents the relationship between LVE shear strain and complex shear modulus (G^*) for GF-based mastics modified with nano-silica (NS-BFM), covering all F/B ratios from 0.6 to 1.2. A consistent decline in LVE strain with increasing G^* was observed, indicating reduced viscoelastic tolerance at higher stiffness. The exponential fit curve followed the trend well, with an R^2 of 0.834 and adjusted R^2 of 0.807, suggesting that nano-silica enhanced viscoelastic behavior, although its predictive accuracy was slightly lower than that of nano-titanium.

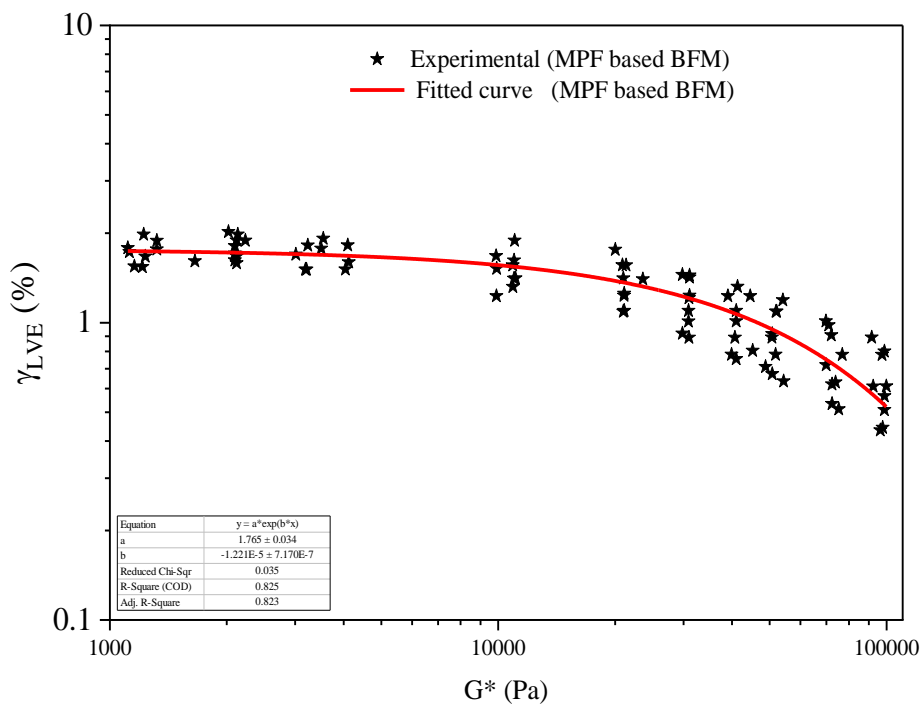


Figure 21 Relation between LVE shear strain and complex shear modulus for GF based bitumen-filler mastics with nano-modifiers.

Figure 21 illustrates the combined performance of GF-based mastics modified with nanoclay, nano-titanium, and nano-silica across the entire F/B range. The data followed a unified exponential decline in LVE strain with increasing G^* , highlighting the consistent stiffening effect. The overall exponential fit achieved a strong R^2 of 0.871 and adjusted R^2 of 0.863, confirming that nano-modifiers collectively contributed to improved linear viscoelastic response and predictable behavior under varying stiffness and filler levels.

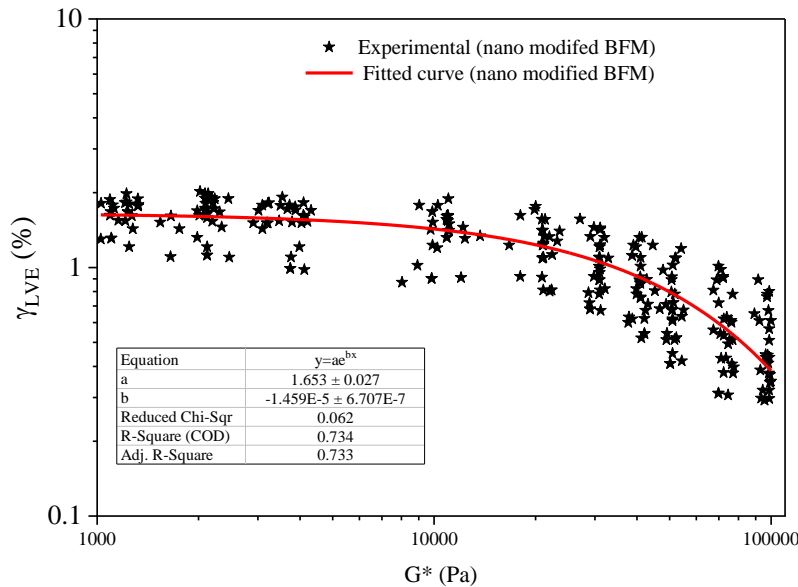


Figure 22. A generalized relation between LVE shear strain and complex shear modulus for bitumen-filler mastics with nano-modifiers.

In overall, figure 22 illustrates a generalized relationship between LVE shear strain and complex shear modulus (G^*) for nano-modified bitumen-filler mastics, combining all three nanoparticle types—nanoclay, nano titanium, and nano silica—with all mineral fillers (MPF, LSF, and GF) across F/B ratios from 0.6 to 1.2. The data exhibited a clear inverse trend, where LVE strain decreased with increasing G^* , highlighting the typical reduction in viscoelastic range as stiffness rose. The exponential fit captured the overall pattern moderately well, with an R^2 of 0.734 and an adjusted R^2 of 0.733. While not highly precise, this curve offers a practical and unified model for predicting viscoelastic behavior across diverse nano-modified mastic compositions, making it a useful tool for performance evaluation in binder design and material selection.

IV. CONCLUSIONS

This study comprehensively examined the linear viscoelastic (LVE) behavior of nano-modified bitumen-filler mastics using three types of mineral fillers (MPF, LSF, and GF) and three nano-additives (nanoclay, nano-titanium, and nano-silica) at varying filler-to-binder (F/B) ratios. The findings consistently demonstrated an inverse exponential relationship between LVE shear strain and complex shear modulus (G^*), indicating reduced viscoelastic range with increasing stiffness. Among the modifiers, nanoclay showed the most significant improvement in LVE performance across MPF systems, while nano-titanium was most effective in LSF and GF systems. The generalized exponential model developed from the data offers a predictive tool for evaluating the viscoelastic behavior of a broad range of nano-modified mastics, supporting optimized material design in asphalt binder applications. The following conclusions were drawn:

- Across all mastics, LVE shear strain decreased exponentially with increasing complex shear modulus, confirming that increased stiffness limits the viscoelastic strain range.
- **Nanoclay Performance:** Nanoclay-modified mastics (NC-BFM) consistently delivered the highest enhancement in LVE behavior, particularly in MPF systems, maintaining a broader viscoelastic range.
- **Nano-Titanium Effectiveness:** Nano-titanium (NT-BFM) showed superior performance in LSF and GF systems, with consistently high R^2 values (~ 0.962), indicating strong reliability in preserving LVE behavior under varying stiffness and filler contents.
- **Generalized Predictive Model:** An exponential model with moderate correlation ($R^2 = 0.734$) was developed to describe the LVE- G^* relationship across all nano-modified mastics, offering a useful tool for predicting viscoelastic behavior in bituminous mixtures.
- **Material Design Implication:** The study highlights the significant role of both filler type and nano-modifier in tailoring the viscoelastic properties of bitumen mastics, enabling more informed design for durable and high-performance pavement materials.

REFERENCES

1. Akbari, A., A. Akbari, A. Ghanbari, and S. Hesami. 2021. "Investigating the influence of aging and filler type on the fatigue behavior of bitumen mastics." *Constr. Build. Mater.*, 26: 121254. Elsevier Ltd. <https://doi.org/10.1016/j.conbuildmat.2020.121254>.
2. Carl, C., P. Lopes, M. Sá da Costa, G. Canon Falla, S. Leischner, and R. Micaelo. 2019. "Comparative study of the effect of long-term ageing on the behaviour of bitumen and mastics with mineral fillers." *Constr. Build. Mater.*, 225: 76–89. Elsevier Ltd. <https://doi.org/10.1016/j.conbuildmat.2019.07.150>.
3. Carneiro, J. O., et al. (2013). "Development of Photocatalytic Asphalt Mixtures by the Deposition and Volumetric Incorporation of TiO_2 Nanoparticles." *Construction and Building Materials*, 38, 594–601. doi:10.1016/j.conbuildmat.2012.09.005.

4. Diab, A., and M. Enieb. 2018. "Investigating influence of mineral filler at asphalt mixture and mastic scales." *Int. J. Pavement Res. Technol.*, 11 (3): 213–224. Chinese Society of Pavement Engineering. <https://doi.org/10.1016/j.ijprt.2017.10.008>.
5. Ezzat, H., et al. (2016). "Evaluation of Asphalt Binders Modified with Nanoclay and Nanosilica." *Procedia Engineering*, 143, 1260–1267. doi: 10.1016/j.proeng.2016.06.119
6. Faramarzi, M., et al. (2015). "Carbon Nanotubes-Modified Asphalt Binder: Preparation and Characterization." *International Journal of Pavement Research & Technology*, 8(1), 29–37.
7. Gong, M., et al. (2018). "Investigating the Performance, Chemical, and Microstructure Properties of Carbon Nanotube-Modified Asphalt Binder." *Road Materials and Pavement Design*, 19(7), 1499–1522.
8. Kale, R., and Meena, C. R. (2012). "Synthesis of Titanium Dioxide Nanoparticles and Application on Nylon Fabric Using Layer by Layer Technique for Antimicrobial Property." *Advances in Applied Science Research*, 3, 3073–3080.
9. Kamboozia, N., Mousavi Rad, S., and Saed, S. A. (2022). "Laboratory Investigation of the Effect of Nano-ZnO on the Fracture and Rutting Resistance of Porous Asphalt Mixture Under Aging Condition and Freeze–Thaw Cycle." *Journal of Materials in Civil Engineering*, 34(5), 04022052.
10. Mansoori, S., and A. Modarres. 2020. "Rheological and micro-structural properties of bituminous mastics containing chemical and wax warm additives." *Constr. Build. Mater.*, 248: 118623. Elsevier Ltd. <https://doi.org/10.1016/j.conbuildmat.2020.118623>.
11. Mazzoni, G., A. Virgili, and F. Canestrari. 2019. "Influence of different fillers and SBS modified bituminous blends on fatigue, self-healing and thixotropic performance of mastics." *Road Mater. Pavement Des.*, 20 (3): 656–670. Taylor & Francis. <https://doi.org/10.1080/14680629.2017.1417150>.
12. Micaelo, R., R. Botella, F. Pérez-Jiménez, and M. Sá da Costa. 2020. "Analysis of the ageing effect on the cyclic tension–compression loading behaviour of bitumen and mastics." *Constr. Build. Mater.*, 243: 118275. Elsevier Ltd. <https://doi.org/10.1016/j.conbuildmat.2020.118275>.
13. Miró, R., A. H. Martínez, F. E. Pérez-Jiménez, R. Botella, and A. Álvarez. 2017. "Effect of filler nature and content on the bituminous mastic behaviour under cyclic loads." *Constr. Build. Mater.*, 132: 33–42. <https://doi.org/10.1016/j.conbuildmat.2016.11.114>.
14. Motevalizadeh, S. M., and K. Mollenhauer. 2024. "Use of multivariate clustering analysis to investigate the physicochemical interactions in bitumen mastics using micromechanical modeling and FTIR spectroscopy." *Constr. Build. Mater.*, 448 (September). Elsevier Ltd. <https://doi.org/10.1016/j.conbuildmat.2024.138230>.
15. Pitroda, J., Jethwa, B., and Dave, S. (2016). "A Critical Review on Carbon Nanotubes." *International Journal of Construction Education and Research*, 2(5), 36–42.
16. Potts, J. R., et al. (2011). "Graphene Oxide: Structural Analysis, Surface Chemistry, and Applications." *Journal of Physical Chemistry C*, 115(33), 13197–13206.
17. Rochlani, M., S. Leischner, G. C. Falla, D. Wang, S. Caro, and F. Wellner. 2019. "Influence of filler properties on the rheological, cryogenic, fatigue and rutting performance of mastics." *Constr. Build. Mater.*, 227: 116974. Elsevier Ltd. <https://doi.org/10.1016/j.conbuildmat.2019.116974>.
18. Santagata, E., O. Baglieri, L. Tsantilis, D. Dalmazzo, and G. Chiappinelli. 2016. "Fatigue and healing properties of bituminous mastics reinforced with nano-sized additives." *Mech. Time-Dependent Mater.*, 20 (3): 367–387. Springer Science+Business Media Dordrecht. <https://doi.org/10.1007/s11043-016-9301-4>.
19. Shabani, A., D. Jelagin, M. N. Partl. 2024. "Advanced testing and characterization of low-temperature cracking in bitumen and mastic." *Mater. Struct. Constr.*, 57 (1): 1–19. Springer Netherlands. <https://doi.org/10.1617/s11527-024-02294-1>.
20. Xing, B., W. Fan, L. Han, C. Zhuang, C. Qian, and X. Lv. 2020. "Effects of filler particle size and ageing on the fatigue behaviour of bituminous mastics." *Constr. Build. Mater.*, 230: 117052. Elsevier Ltd. <https://doi.org/10.1016/j.conbuildmat.2019.117052>.

Copyright & License:



© Authors retain the copyright of this article. This work is published under the Creative Commons Attribution 4.0 International License (CC BY 4.0), permitting unrestricted use, distribution, and reproduction in any medium, provided the original work is properly cited.